Journal of Glaciology, Vol. 22, No. 86, 1979

APPLICATION OF NUMERICAL TRANSIENT FLUID DYNAMICS TO SNOW AVALANCHE FLOW. PART II. AVALANCHE MODELING AND PARAMETER ERROR EVALUATION

By T. E. LANG

(Department of Civil Engineering and Engineering Mechanics, College of Engineering, Montana State University, Bozeman, Montana 59715, U.S.A.)

and M. MARTINELLI, JR

(Rocky Mountain Forest and Range Experiment Station, 240 West Prospect Street, Fort Collins, Colorado 80521, U.S.A.)

ABSTRACT. Under evaluation is the range of the parameters of internal viscosity and surface friction of flowing avalanches in order to represent the flow numerically by computer program AVALNCH. Nominal values of these parameters are determined to be in the range 0.4 to 0.6 for snow flowing on snow, with values as high as 0.8 to 0.9 for snow flowing on rough ground. Using a nominal avalanche path, the basic parameters: (1) depth of initial release slab, (2) viscosity and friction, (3) adverse grade, and (4) flow spreading are determined to be in the order listed as regards their relative effect on avalanche runout distance. Program AVALNCH, which permits treatment of flow parameters separately from geometric parameters, provides a versatile tool for the prediction of avalanche runout, as well as for related studies of avalanche dynamics.

RÉSUMÉ. *Application du calcul numérique d'écoulement en dynamique des fluides a l'écoulement d'une avalanche de neige Partie II. Simulation des avalanches et l'évaluation de l'erreur des paramètres.* Il s'agit d'évaluer l'ordre de grandeur des paramètres de viscosité interne et de frottement superficiel des avalanches en mouvement en vue de représenter numériquement l'écoulement pour le programme informatique AVALNCH. Les valeurs nominales de ces paramètres ont été déterminé comme étant dans la fourchette de 0,4 à 0,6 pour la neige coulant sur la neige et atteignant jusqu'à 0,8 à 0,9 pour de la neige coulant sur un sol rugueux. En utilisant un couloir d'avalanche donné, on a examiné les paramètres de base: (1) épaisseur de la plaque de départ initiale, (2) viscosité et friction, (3) contrepentes et (4) étalement du courant et on a constaté qu'ils influaient dans cet ordre sur la distance d'arrêt de l'avalanche. Le programme AVALNCH, qui permet un traitement séparé des paramètres internes de l'écoulement et des paramètres géométriques, constitue un outil souple de prévision de la zone de dépôt, aussi bien que pour les études rapportées de dynamique de l'avalanche.

ZUSAMMENFASSUNG. *Anwendung der numerischen Dynamik nichtstationärer Strömungen auf den Lawinenabgang. Teil II. Modellbildung für Lawinen und Auswertung von Parameterfehlern.* Zur numerischen Erfassung des Lawinenabgangs mit dem Rechenprogramm AVALNCH wird der Bereich der Parameter für die innere Viskosität und die Oberflächenreibung untersucht. Nennwerte für diese Parameter lassen sich im Bereich 0,4 bis 0,6 für den Fluss von Schnee auf Schnee und im Bereich 0,8–0,9 für den Fluss von Schnnee auf rauhem Untergrund bestimmen. Für eine bestimmte Lawinenbahn werden die Grundparameter (1) Dicke der Abbruchschicht, (2) Viskosität und Reibung, (3) Gegensteigung und (4) Fliessausbreitung in der Rangordnung ohres relativen Einflusses auf die Reichweite der Lawine bestimmt. Das Programm AVALNCH, das die Behandlung von Fliessparametern unabhängig von geometrischen Parametern gestattet, stellt ein vielseitiges Mittel sowohl für die Vorhersage von Lawinenreichweiten wie für verwandte Studien zur Lawinendynamik dar.

INTRODUCTION

In Part I of this report (Lang and others, 1979) a simple geometry was evaluated in order to establish a range for the flow parameters of surface friction and internal viscosity.

In the absence of experimentally measured data for these parameters, we now have recourse to event modeling to establish more specific limits to their values. The magnitudes of these parameters are undoubtedly influenced by the size of snow blocks in the flow, the type of snow in the release slab, the type of snow in the avalanche track, the speed and speed history of the moving mass, the antecedent weather conditions and snow type changes along the path, local terrain anomalies, and many other conditions unique to each avalanche path. The enormity of the problem of developing a complete characterization of an avalanche path suggests that, in any gross averaging of viscosity and surface friction, only a "worst case" response can be estimated.

To this end, a number of specific avalanche incidents for which the gross response characteristics are known are analyzed. In addition to a consideration of simple flow models, interest also centers on modeling road cuts, variable friction paths, constricting and expanding flows, and the effect of obstacles and adverse grade on flow. The dominant parameters that influence the velocity and runout distance of flow can be identified by numerical investigation as: (1) the depth of the initial release slab, (2) the viscosity and surface friction values, (3) an adverse grade, and (4) the terminal flow spreading angle. An error analysis of these parameters is performed in order to establish their relative importance for accurate modeling of flow. An alternative aim in establishing parameter sensitivity is that of providing guidance for those future field experiments designed to isolate and measure the more important factors which influence avalanche flow.

Avalanche path analyses

A number of avalanche paths are selected for modeling in order to consider the various conditions that can occur on different paths. For example, a roadcut or adverse grade may interrupt an otherwise smooth runout. A roadcut may also cause a flowing avalanche to revert to a powder avalanche by deflecting the flow upward and entraining air. This can be represented in program AVALNCH by reducing the values of ν and f_0 on the basis of available physical data.

Another factor is the contraction or expansion of path widths, one example of which is the terminal fanning of the flow which often occurs. These and other detailed considerations are evaluated in the following examples. For brevity, only the longitudinal profile and brief comments on each path are cited here. For a more complete description of these cases, see Lang and others (1978).

Case 1. Pallavicini avalanche path

The longitudinal profile of the Pallavicini avalanche path (Loveland Pass 7.5 ft Quadrangle, Colorado) path is shown in Figure 1. The starting zone is steep for the first 80 m, and then becomes less steep for the remaining 850 m to the valley floor. Exceptional avalanches with significant air-borne contents are known to reach the road—a travel distance of 940 m (cell 105 in Fig. 1). (Travel distance is the horizontal distance from the face of the avalanche crown to the end of the debris.) Most small midwinter avalanches stop between the grade change at 400 m (cell 48) and the creek (cell 96). The flow path is divided into cells 10.0 m long, and the avalanche starting zone is assumed to be 50 m in length. Table I is a summary of the various computer runs made using AVALNCH.

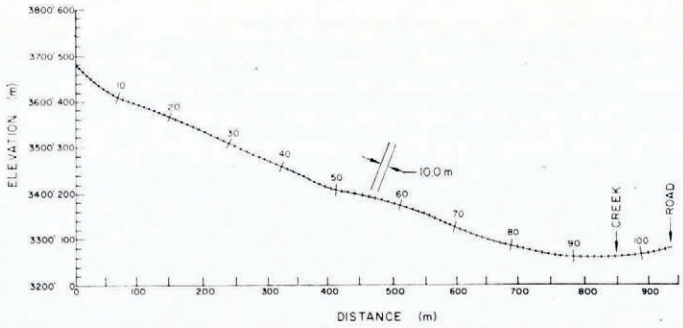

Fig. 1. Longitudinal profile of Pallivicini avalanche path.

https://doi.org/10.3189/S002214300001409X Published online by Cambridge University Press

For an avalanche of height 0.75 m, the flow terminates rapidly for viscosity and friction values of 0.55. What might be considered a nominal avalanche height of 0.75 m occurs when ν and f_0 are set to 0.5. Under these conditions, the avalanche reaches cell 53, a point on a local bench of the profile. Flow of a 2.0 m high avalanche slab with $\nu = f_0 = 0.5$ (run 8, Table I) ends 40 m beyond the creek, but does not reach the road. It is necessary to reduce ν and f_0 to 0.4 for an avalanche 2.0 m high to reach the road (run 10). This indicates that a deep, dry avalanche with an airborne phase is modeled with the parameters ν and f_0 set to approximately 0.4.

TABLE I. TRAVEL DISTANCE OF THE PALLAVICINI AVALANCHE FOR DIFFERENT FLOW HEIGHTS AND DISSIPATION

Run number	*Viscosity* $m^2 s^{-1}$	*Friction coefficient*	*Initial height of slab* m	*Travel distance* m	*Comments*
1	0.55	0.55	0.75	130	Avalanche stops in cell 17. Maximum debris depth is 0.7 m and covers 80 m of slope
2	0.50	0.50	0.75	440	Avalanche stops in cell 53. Maximum debris depth is 0.6 m and covers 130 m of slope
3	0.50	0.50	1.00	780	Avalanche stops at cell 90. Maximum depth 1.0 m; extent 100 m. Initial slab 40 m extent
4	0.60	0.60	1.00	710	Avalanche stops in cell 82. Maximum debris depth is 0.8 m and covers 170 m of slope
5	0.50	0.50	1.50	860	Avalanche stops at cell 97, 10 m beyond creek. Maximum depth 3.0 m. Extent 40 m
6	0.60	0.60	1.50	850	Avalanche stops at creek (cell 96). Maximum debris depth is 1.5 m and covers 60 m of slope
7	0.60	0.60	2.00	870	Avalanche stops at cell 98 just beyond creek. Maximum debris depth 7.4 m. Avalanche covers 40 m of slope
8	0.50	0.50	2.00	890	Avalanche stops at cell 100. Maximum depth 3.6 m. Extent 40 m. Adverse slope is effective
9	0.45	0.45	2.00	910	Avalanche stops at cell 102. Maximum depth 9.0 m. Extent 40 m
10	0.40	0.40	2.00	—	Avalanche leaves grid at cell 105 with velocity of 5.0 m s^{-1}

Case 2. Stanley avalanche path

The Stanley avalanche path (Berthoud Pass Quadrangle, Colorado) crosses a highway twice and has two possible starting zones (Fig. 2). Most avalanches released at starting zone 2 stop at or above the upper highway. Most large avalanches released at starting zone 1

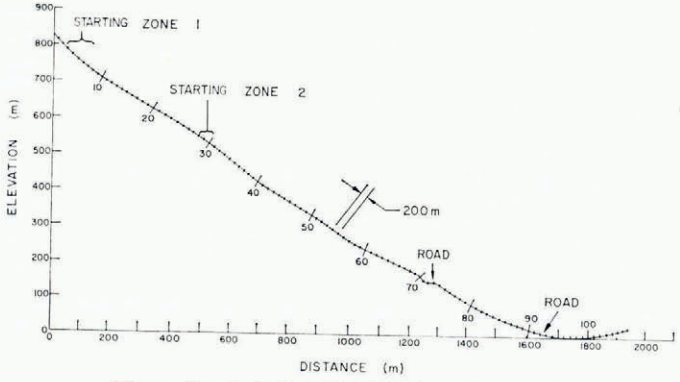

Fig. 2. Longitudinal profile of Stanley avalanche path.

https://doi.org/10.3189/S002214300001409X Published online by Cambridge University Press

stop in the reach between the two highway crossings. The slope above the upper road crossing is almost uniform except for a small grade increase at starting zone 1.

The major interest here is in producing a model for the upper road which will represent adequately the different types of flow. The upper road is three lanes wide with a turnout, which is equivalent to one cell 20 m long. Two additional cells with zero slope are, therefore, placed to represent the up-hill highway cut and the snowplow embankment on the down-hill

TABLE II. TRAVEL DISTANCE OF STANLEY AVALANCHE FOR DIFFERENT SPECIFIED FLOW CONDITIONS

Run number	*Starting zone*	*Viscosity* $m^2 s^{-1}$	*Friction coefficient*	*Initial height of slab* m	*Maximum velocity* $m s^{-1}$	*Cell number*	*Travel distance* m	*Cell number*	*Comments*
1	1	0.55	0.55	1.0	9	15	800	74	Initial 40 m slab stops in upper road; 1.3 m maximum depth; extent 100 m; upper road $f_0 = 0.55$
2	2	0.60	0.60	1.0	8	34	770	73	Initial 40 m slab stops in upper road; 1.1 m maximum depth; extent 160 m; upper road $f_0 = 0.6$
3	2	0.55	0.55	1.0	10	34	800	74	Initial 100 m slab stops in upper road; 1.8 m maximum depth; extent 280 m; upper road $f_0 = 0.55$
4	1	0.55	0.55	1.5	22	10	1 600	90	Initial 60 m slab stops between roads; 0.5 m maximum depth; extent 320 m; upper road $f_0 = 0.9$; velocity across road = 5 $m s^{-1}$ then = 13 $m s^{-1}$
5	1	0.55	0.55	2.0	28	10	1 780	99	Initial 60 m slab stops past second road; 7.3 m maximum depth; extent 20 m; upper road $f_0 = 0.9$; velocity across road = 23 $m s^{-1}$
6	1	0.55	0.55	2.0 tapered to 1.0	28	74	1 780	99	Initial 100 m slab stops past second road; 8.6 m maximum depth; extent 20 m; upper road $f_0 = 0.55$; velocity across road = 23 $m s^{-1}$
7	1	0.55	0.55	2.0	28	74	1 780	99	Initial 60 m slab stops past second road; 8.6 m maximum depth; extent 20 m; upper road $f_0 = 0.55$; velocity across road = 26 $m s^{-1}$
8	1	0.55	0.55	2.5 tapered to 1.0	45	75	1 820	101	Initial 100 m slab stops past second road; 9.0 m maximum depth; extent 20 m; upper road $f_0 = 0.55$; velocity across road = 45 $m s^{-1}$
9	1	0.55	0.55	3.0 tapered to 0.0	60	78	Flows out of grid		Initial 100 m slab flows out of grid at $V = 37$ $m s^{-1}$; upper road $f_0 = 0.55$; velocity across road = 59 $m s^{-1}$

https://doi.org/10.3189/S002214300001409X Published online by Cambridge University Press

side. These three cells, plus one additional cell on each side of the road are given large friction values ($f_0 = 0.9$) to simulate the road, the embankments, and the irregular snow profile in the vicinity of the road. For the remainder of the path, typical snow coefficient values for midwinter hard pack are assumed with $\nu = f_0 = 0.55$.

Results from several "typical" avalanche runs are listed in Table II. One-meter-deep avalanches starting in zone 2 are trapped at the upper road, this is consistent with a number of sightings. Run 4, for a 1.5 m deep avalanche starting in zone 1, barely passes the upper road, then regains speed but stops later between the roads, another observed result. When the avalanche depth is increased to 2.0 m and the avalanche is initiated in zone 1, the avalanche crosses the lower road. Tapered starting profiles, 2.5 and 3.0 m deep at the crown and 1.0 m deep 100 m down-slope at the toe, behave in the same way as the avalanche with a uniform depth of 2.0 m.

A field observation of 4 March 1977 showed that a control-released avalanche from starting zone 1 reached a speed of 33 m s^{-1} above the upper road. Most debris stopped at the upper road (cells 70–73) with a small amount reaching cell 85. The average fracture face height was 1.51 m and the average slab height in the starting zone was 1.19 m. The computation that best matches these observations is run number 4 in Table II. The greatest discrepancy is in the two velocity values, this is partially attributable to differences in the slab height, and to possible parallax errors in the field estimates of velocity.

Comparing runs 1 and 3, and 5 and 6, we conclude that the length of the starting slab does not change the flow limits significantly. Flow length could be important when the leading part of the flow fills a recess (road cut, creek recess, etc.) and the flow is long enough for the trailing part to flow over the filled recess. This phenomenon cannot be modeled exactly by AVALNCH, except that the recess can be filled by changing the profile of the path before starting the computer run. The upper road intrusion modeled for Stanley is apparently sufficient to stop the smaller avalanches, and yet it permits the larger ones to flow beyond the road. User judgement is needed when setting up these intrusion models for each separate case.

Finally, it should be noted that on the near-uniform slope in release zones 1 and 2, the avalanche velocity for the 1.0 and 1.5 m avalanches approximates to the condition, quoted by Voellmy (1955), that flow velocity reaches 80% of maximum speed after the avalanche has covered a distance equal to 25 times the initial slab depth. An alternate statement of this observation is that the avalanche accelerates rapidly at the start and then flows on at a rate close to equilibrium if the slope is constant. This physical condition is often observed in AVALNCH results.

Case 3. Max's Mountain avalanche path

The Number 3 East avalanche path (Seward D-6 Quadrangle, Alaska) off "Max's Mountain" (identified on map as Baumann Bump), which is 64 km south-east of Anchorage, Alaska, is shown in profile in Figure 3.

The avalanche path is represented by 129 cells parallel to the slope, each 10 m long. There are several rapid changes in elevation along the path, these allow us to check how well AVALNCH can handle such an uneven slope. Snow conditions are also unique, with dry snow often found at elevations of approximately 400 m, and wet, viscous snow below this elevation. All avalanches observed in the past several years have stopped on the slope or have been trapped in the gully at cell 116 with no flow onto the gun-tower bench.

Two runs were made in order to model the different conditions known to occur on this slope. In both cases, slab dimensions are set to 1.5 m depth and 40 m in extent. For run 1, a large viscosity ($\nu = 0.7$) is assigned to the slab to simulate wet snow in the starting zone. Friction is set at $f_0 = 0.7$ from the starting zone to cell 80, and $f_0 = 0.9$ to cell 129; this models moderate friction in the upper path and large friction in the lower (coastal) zone.

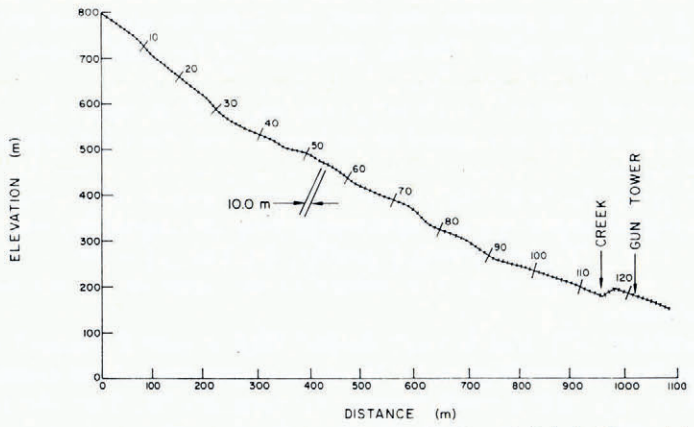

Fig. 3. Longitudinal profile of number 3 east avalanche path (Max's Mountain).

Results show that this avalanche enters cell 115 at a leading-edge speed of 10 m s^{-1}, and stops in cell 116. The debris is scattered over 120 m to a depth of 0.94 m in cell 116. The maximum velocity attained by the avalanche is 20 m s^{-1} at cell 12.

In run 2 viscosity was set at a midwinter value of $\nu = 0.55$ for dry snow. Friction was assumed to have a nominal value of $f_0 = 0.5$ up to cell 72, $f_0 = 0.7$ from cell 73 to cell 80, and $f_0 = 0.9$ for the remainder of the path. This is intended to simulate dry-release snow running on a dry upper path but onto wet snow in the lower path. Results of this run are a maximum speed of 27 m s^{-1} at cell 33, with snow entering cell 115 at 10 m s^{-1}, and stopping in cell 116. Debris covers 90 m, to a maximum depth of 1.4 m in cell 116.

The conclusions which may be drawn from this example are that AVALNCH shows numerical stability even for cases where the gravitational components g_x and g_y vary rapidly or change sign. For the two flow conditions described above, the adverse grade in the runout zone is more important in determining runout distance than are frictional values along the track. The Max's Mountain path is a good example of a formulation in which there are good physical reasons for varying the friction values along the path.

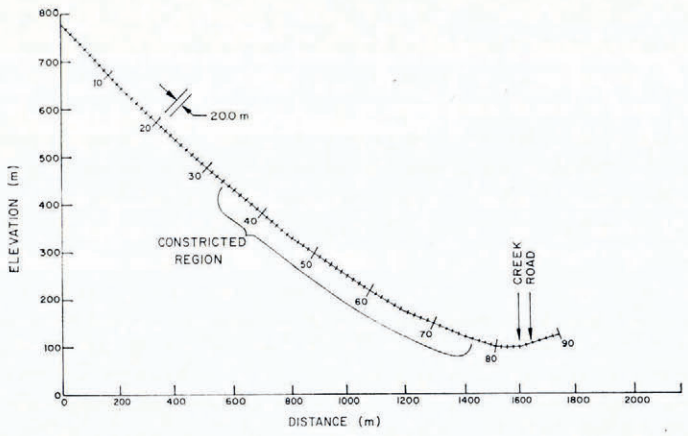

Fig. 4. Longitudinal profile of Imogene avalanche path.

https://doi.org/10.3189/S002214300001409X Published online by Cambridge University Press

Case 4. Imogene avalanche path

The Imogene profile (Silverton Quadrangle, Colorado; Fig. 4) is modeled by 90 cells each 20 m in length. Initial flow height is 1.5 m and the extent of the starting slab along the fall line is 100 m. Viscosity is set at $\nu = 0.5$. A region of constriction from cell 30 through 51 is modeled by three different friction values.

Run 1. Friction is set at $f_0 = 0.5$ over entire path. Flow velocity is found to be maximum at 26 m s^{-1} in cell 16 and decreases until flow stops in cell 85, midway between the creek and the road. Debris extends over 140 m with a maximum depth of 5.5 m. The leading-edge velocity at the exit from the constricted region is 20 m s^{-1}.

Run 2. Friction is increased to 0.6 in the constricted region. Flow stops in cell 85, with debris spread over 160 m, to a maximum depth of 5.5 m. The leading-edge velocity from the constricted region is 17 m s^{-1}, a decrease of 15% compared with run 1.

Run 3. Friction is decreased to 0.4 in the constricted region. Leading-edge velocity from the constricting region is 24 m s^{-1} (20% increase over that of run 1), the flow stops in cell 85, with debris spread over 140 m, with a maximum depth of 5.6 m.

Cell 85 is the first cell of the adverse grade in the runout zone, and its effect apparently controls the flow more than do the adjustments made to friction in the constricted region. In the fluid dynamics of water, surface friction in regions of constriction decreases in importance because flow depth increases, and viscosity increases in importance because circulation increases. However, with no information known for snow, no conclusions on this point can be reached. A previous observation that ν and f_0 have approximately equal influence suggests that in the case of a constriction, no adjustment need be made.

In further evaluation of this problem, AVALNCH has been modified to account for variable width of the flow. The modification is a pseudo-simulation of three-dimensional flow in which the two-dimensional flow height of each cell is adjusted each CYCLE of iteration to account for local changes in flow width. This approximation is not a complete three-dimensional formulation, for which height variation along a contour would be allowed. However, it will account for large variations in width, consistent with the accuracy to be expected when calculations are based upon the nominal slope and material properties we are currently able to establish for flowing snow.

For the variable-width program, additional input includes a width factor W(I) for each cell that can be read directly from a topographic map. One approach to setting the width factors is to select a value of unity in the starting zone and then to adjust it for down-slope cells as the width of the avalanche-track changes. In representing width changes, even abrupt changes, the factors should vary gradually, since snow entrapment will smooth even the most irregular boundaries.

To accommodate increases in height of the flow in AVALNCH due to a constriction, it is necessary to include more than one row of cells above the row in which the avalanche initially flows.

The variable-width approximation for the Imogene avalanche path is depicted by the heavy solid lines drawn in Figure 5. The shaded region is the assumed extent of the snow mass of the starting zone. The dashed lines are the assumed boundaries of the flow of the shaded mass after release.

Results of the variable flow calculation show that the flowing snow emerges from the constricted region of the path at a speed of approximately 23 m s^{-1} and stops in cell 85. Thus, run 3 of the constant-width cases is duplicated approximately. Cell 85 is the first cell of adverse grade in the Imogene path, after flow crosses the creek bed, and is significant in stopping the avalanche. Thus, a more meaningful number for comparison of the different runs is the

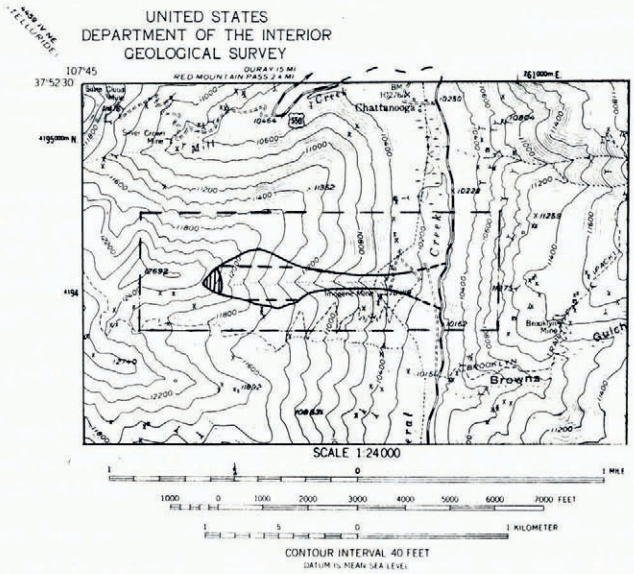

Fig. 5. Topographic map of avalanche path Imogene from which geometric path data were taken.

leading-edge velocity of the flow entering cell 85. Leading-edge velocity and final maximum debris height are listed in Table III for the three constant-width flow runs and the variable-width flow runs. The reported velocity is the average of the velocities computed for cells 80 through 84, which, by averaging, reduces local computational variations. We conclude from these results that the overall effect of the modeling assumptions on terminal flow is small, compared to the influence of terminal-zone geometry. Significant variation in snow-debris height is noted, and is attributed to the number of active cells used in the vertical range of the grid. For consistent results, one cell height should be maintained between the cell of maximum flow height and the upper boundary cell at all points along the path. If the restriction requiring accurate prediction of debris height is removed, then all models predict terminal velocities with an accuracy that is comparable to the limits encountered in selecting values for ν and f_0.

TABLE III. SUMMARY OF LEADING EDGE TERMINAL VELOCITY AND MAXIMUM DEBRIS HEIGHT FOR IMOGENE PATH OF AVALANCHE

Run number	*Description of numerical simulation in computer run*	*Average flow velocity into cell 85* m s^{-1}	*Maximum height of snow debris* m
1	Constant-width flow. Friction $f_0 = 0.5$ over path, and $f_0 = 0.4$ in constriction region. Two-cell-height model of flow regime	10.98	5.6
2	Constant-width flow. Friction $f_0 = 0.5$ over entire path. Two-cell-height model of flow regime	10.74	5.5
3	Constant-width flow. Friction $f_0 = 0.5$ over path, and $f_0 = 0.6$ in constriction region. Two-cell-height model of flow regime	10.68	5.5
4	Variable-width flow. Friction $f_0 = 0.5$ over entire path. Three-cell-height model of flow regime	11.9	2.9
5	Variable-width flow. Friction $f_0 = 0.5$ over entire path. Four-cell-height model of flow regime	12.9	3.1
6	Variable-width flow. Friction $f_0 = 0.5$ over entire path. Five-cell-height model of flow regime	12.9	3.2

Avalanche parameter error analysis

Results are reported from experiments carried out with the Ironton Park avalanche path (see Part I of this report; Lang and others, 1979). The runout of this path is onto a flat frozen lake surface. This path was selected for computer alteration because of its simple geometry, in order to assess the sensitivity of different parameters on the flow. Among parameters considered are: (1) depth of the initial released slab, (2) friction and viscosity of the flow, (3) adverse grade in runout, and (4) spreading angle of the runout. The depth, friction, and viscosity parameters have already been evaluated by the results reported in Part I. Adverse grade and terminal spreading of the flow remain to be evaluated. These are introduced separately into the Ironton Park runout by representing their effect artificially. For example, although an actual avalanche would not spread appreciably on the flat, numerical spreading is introduced in the computer model without introducing the attendant slope roll-off which must actually produce the phenomenon. The effect of adverse grade is likewise modeled by simple specification of gravity components to replace those corresponding to the lake surface.

We arbitrarily select a nominal set of values for the different parameters, then vary the specific parameter, first by 20% and then by 40%, and note the change in runout distance. Spreading angle is set nominally at $\phi = 10°$, adverse grade at 5%, viscosity and friction at 0.5, and slab starting depth at 2.0 m. Results of these computations are shown in Figure 6. It is noted there is a non-linear relation between the parameters and runout distance. An attempt is made to select values that do not lie on either a flat or a steep portion of any curve. The intention, then, is to establish order-of-magnitude estimates of the relative importance of the parameters for a simple avalanche path. That this goal has been achieved is indicated in the results of Figure 6. The depth of the slab that is initially released has the greatest effect on runout distance, with a 30% variation in depth resulting in a 70% change in runout distance. This is followed by viscosity or friction values, in which a 30% change in the parameter results in a 45% change in runout distance. An adverse slope change of 30% corresponds to 25% change in runout distance, and a 30% change in spreading angle amounts to

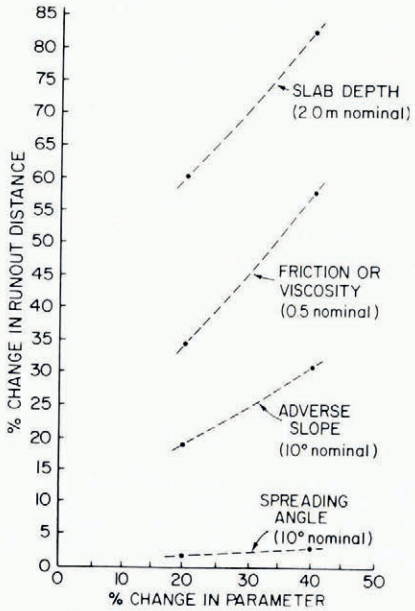

Fig. 6. Change in runout distance as a function of changes in various flow parameters for the Ironton Park avalanche.

https://doi.org/10.3189/S002214300001409X Published online by Cambridge University Press

only about a 2% change in runout distance. One parameter not reported in Figure 6 is the length of snow slab (parallel to the slope) released, but it had been previously determined to have negligible effect on runout distance (Stanley avalanche path, Case 2).

The primary conclusion we draw from these results is that the parameters of adverse grade and spreading angle, which can most readily be evaluated from topographic maps, have the least influence on runout distance. The parameters of slab depth, friction, and viscosity of the flow, which have the greatest effect on runout, are more difficult to evaluate and deserve special attention in future avalanche-measurement projects.

Summary and conclusions

For snow flowing on snow, surface friction and viscosity are in the range 0.55 to 0.60 for wet or heavy dry snow, 0.5 to 0.55 for lighter hard-packed snow, and less than 0.5 for light dry snow with perhaps an air-borne phase. Values of friction greater than 0.6 and up to 0.85 or 0.9 may be used in modeling the roughness of rocky ground or the drag of wet viscous snow.

An error analysis shows that height of the initial-release slab is the most important factor influencing avalanche-runout distance with viscosity and surface friction, slope of adverse grade, and terminal spreading angle in decreasing order of importance.

The influence of constriction and expansion regions of flow geometry is modeled by a pseudo-three-dimensional representation; however, the refinement in this option does not appear to be worth the increase in computer cost, except in the case where distribution of the terminal debris is important. The length, parallel to the slope, of the release slab is determined to have small effect on runout distance, but may have an important effect on avalanche flow over road cuts and obstacles. A simplistic approach is taken to modeling road cuts and embankments and further experimental verification is clearly warranted. In particular, field evidence of local flow behavior when an avalanche interacts with these perturbative intrusions would help to establish an analytic approach to the problem.

The ability of AVALNCH to separate path-geometry effects from dissipative effects makes it a versatile tool for the analysis of runout distance and other avalanche dynamic problems. For example, it should aid in the prediction of the effects of avalanche impact with structures, the treatment of tributary flow problems, the assessment of the snow-entrainment phenomenon in many avalanche flows, and other related problems associated with snow in motion.

Acknowledgement

This study was carried out as part of a co-operative agreement between Rocky Mountain Forest and Range Experiment Station of the U.S. Forest Service, Fort Collins, Colorado and the Department of Civil Engineering and Engineering Mechanics, Montana State University, Bozeman, Montana.

MS. received 21 December 1977

REFERENCES

Lang, T. E., *and others*. 1978. Numerical hydrodynamic simulation of snow avalanche flow, by T. E. Lang, K. L. Dawson and M. Martinelli, Jr. *U.S. Forest Service. Research Report* RM 205.

Lang, T. E., *and others*. 1979. Application of numerical transient fluid dynamics to snow avalanche flow. Part I. Development of computer program AVALNCH, by T. E. Lang, K. L. Dawson and M. Martinelli, Jr. *Journal of Glaciology*, Vol. 22, No. 86, p. 107–15.